NIH Public Access
Author Manuscript
Cancer Res. Author manuscript; available in PMC 2010 March 15.

Published in final edited form as:
Cancer Res. 2009 March 15; 69(6): 2375–2383. doi:10.1158/0008-5472.CAN-08-3359.

Mitochondrial Dysfunction and Reactive Oxygen Species Imbalance Promote Breast Cancer Cell Motility through a CXCL 14-Mediated Mechanism

Helene Pelicano, **Weiqin Lu**, **Yan Zhou**, **Wan Zhang**, **Zhao Chen**, **Yumin Hu**, and **Peng Huang**
Department of Molecular Pathology, The University of Texas M. D. Anderson Cancer Center, Houston, Texas

Abstract

Although mitochondrial dysfunction and reactive oxygen species (ROS) stress have long been observed in cancer cells, their role in promoting malignant cell behavior remains unclear. Here, we show that perturbation of the mitochondrial respiratory chain in breast cancer cells leads to a generation of subclones of cells with increased ROS, active proliferation, high cellular motility, and invasive behaviors *in vitro* and *in vivo*. Gene expression analysis using microarrays revealed that all subclones overexpressed CXCL14, a novel chemokine with undefined function. We further show that CXCL14 expression is up-regulated by ROS through the activator protein-1 signaling pathway and promotes cell motility through elevation of cytosolic Ca^{2+} by binding to the inositol 1,4,5-trisphosphate receptor on the endoplasmic reticulum. Abrogation of CXCL14 expression using a decoy approach suppressed cell motility and invasion. Our data suggest that mitochondrial dysfunction and ROS stress promote cancer cell motility through a novel pathway mediated by CXCL14.

Introduction

Emerging lines of evidence suggest that cancer cells may have mitochondrial dysfunction and adapt aerobic glycolysis to generate ATP. The involvement of reactive oxygen species (ROS) signaling in tumor metastasis has also been recognized (1,2). ROS are constantly generated during cellular metabolism, particularly through the mitochondrial respiration, and exert various physiologic actions (3,4). Oxidative stress is a state of redox imbalance caused by increased ROS generation, decreased antioxidant capacity, or both. Recent studies suggest that cancer cells, compared with the normal cells, are under increased oxidative stress associated with oncogenic transformation, alterations in metabolic activity, and increased generation of ROS (5–7). The increased ROS in cancer cells may in turn affect certain redox-sensitive molecules and further lead to significant consequences such as stimulation of cellular proliferation, cell differentiation, alterations in sensitivity to anticancer agents, promotion of mutations and genetic instability, and contributing to carcinogenesis (5,8–11). The accumulation of certain genomic mutations enables cells to further acquire the ability to proliferate, generate a tumor, and eventually metastasize (12).

© 2009 American Association for Cancer Research.

Requests for reprints: Peng Huang, Department of Molecular Pathology, Unit 951, The University of Texas M. D. Anderson Cancer Center, 1515 Holcombe Boulevard, Houston, TX 77030. Phone: 713-834-6044; Fax: 713-834-6084; E-mail: phuang@mdanderson.org.

Note: Supplementary data for this article are available at Cancer Research Online (http://cancerres.aacrjournals.org/).

Disclosure of Potential Conflicts of Interest
No potential conflicts of interest were disclosed.

NIH-PA Author Manuscript
NIH-PA Author Manuscript
NIH-PA Author Manuscript

NIH-PA Author Manuscript

NIH-PA Author Manuscript

NIH-PA Author Manuscript

Mitochondria are major sites of ROS generation, which occurs mainly at complexes I and III of the respiratory chain. ROS production increases when electron transport function is compromised, leading to increased leakage of electrons, which react with oxygen to form superoxide. The molecular mechanisms involved in the mitochondrial dysfunction and increased ROS production are not well understood. Multiple pathways may converge in mitochondria to modify respiratory chain activity. Moreover, recent studies indicate that the production of ROS may be accompanied by changes in mitochondrial metabolism (13). The production of excess superoxide can cause oxidative DNA damage and genomic instability (14), transformation of cells in culture (8), and potentiate tumor progression (11). In fact, mitochondrial DNA (mtDNA) is highly susceptible to damage because it is not protected by histones and is directly exposed to ROS generated by the respiratory chain. Moreover, DNA repair capacity is less efficient in the mitochondria. These factors might explain why human cancers have high levels of mtDNA mutations.

Since Warburg proposed the cancer “respiration injury” theory (15), mitochondrial alterations in cancer cells have been intensively studied to understand their role in tumor development, ROS generation, and carcinogenesis (16,17). Despite significant progress in this research area, little is known of the alterations in mitochondrial structure and function that contribute to cell mobility and metastasis, especially in breast cancer cells. Here we report that perturbation of mitochondrial respiration in breast cancer cells leads to redox alterations and more invasive behaviors, which seem to be mediated by elevated cytosolic calcium through a novel ROS→activator protein-1 (AP-1)→CXCL14 pathway.

Materials and Methods

Reagents

[^{3}H]Deoxyglucose and [γ-^{32}P]ATP were acquired from Amersham Pharmacia Biotech. Recombinant human active CXCL14 and CXCL14 antibody were obtained from R&D Systems. GRP78 and heat shock protein 60 antibodies were from Santa Cruz Biotechnology, Inc., and inositol 1,4,5-triphosphate receptor (IP_3R) antibody from BD Biosciences. SP600125 was acquired from AG Scientific, Inc. CM-H_2DCF-DA, dihydroethidium (Het), Calcium Green-1, MitoTracker Green, Fluo-3, ER-Tracker Blue-White DPX, rhodamine-123, and ionomycin were purchased from Invitrogen/Molecular Probes. Phosphorothioate decoy oligo specific for AP-1 (5′-CACTCGGTGACTCACTGAGATTTAAAAAAAATCTCAGTGAGTCACCGAGTGGTTCTGCATA-3′) and phosphorothioate scrambled oligo (5′-GCATGGACTGTATCGGAAAAACGATACAGTCCATGCCATTATA-3′) were synthesized by Sigma Genosys. The 2 bases at the 3′ and 5′ ends are phosphorothioates. Human CXCL14 cDNA clone was from Origene Technologies, Inc.

Cell culture and migration/invasion assays

MCF7 and its subclones were cultured in DMEM-F12 medium (Cellgro, Mediatech, Inc.) supplemented with 10% fetal bovine serum and 2 mmol/L glutamine at 37°C with 5% CO_2. Cell migration and invasion assays were done using chambers with 8-μm-porosity polycarbonate filter membranes according to the manufacturer’s instructions (Becton Dickinson Labware). Cells that invaded to the lower surface were stained with Fisher Diagnostics Hema 3 Staining System (Thermo Fisher Scientific, Inc.) and photographed under a microscope (Eclipse TS100, Nikon) at ×20 magnification.

Chromatin immunoprecipitation assay

The chromatin immunoprecipitation assay kit from Upstate was used for this study. Protein-DNA complexes were immunoprecipitated with AP-1 antibody (Santa Cruz Biotechnology).

NIH-PA Author Manuscript

NIH-PA Author Manuscript

NIH-PA Author Manuscript

PCR was done using 2 AL of DNA sample with primers 5′-GGCGACGGGCGGGCTGGGAAG-3′ (forward) and5′-GGAGACGCCACCCAGCTCTG-3′ (reverse) to amplify region −323/−83 of the *CXCL14* promoter. Amplification of soluble DNA before immunoprecipitation was used as an input control. All chromatin immunoprecipitation experiments were repeated at least three times.

Measurements of respiration, glucose uptake, lactate production, ROS, mitochondrial mass, mitochondrial membrane potential, and calcium

Oxygen consumption, cellular glucose uptake, lactate production, mitochondria mass, ROS content, and mitochondrial transmembrane potential ($\Delta\psi_m$) were measured as previously described (18,19). To measure cellular Ca^{2+}, cells were stained with 3 μmol/L Calcium Green-1 in serum-free medium for up to 1 h and analyzed using a FACScan flow cytometer (Becton Dickinson Bioscience). Cells were loaded with 200 nmol/L ER-Tracker Blue-White DPX to measure endoplasmic reticulum (ER) Ca^{2+} under UV excitation, using a LSRII flow cytometer (Becton Dickinson) equipped with a 350-nm excitation laser and a 530-nm centered band-pass filter, as previously described (20).

Nuclear extract and gel shift assay

EMSA analysis was done using the Gel Shift Assay System (Promega), according to the manufacturer's instructions, with human recombinant AP-1 (c-jun) and 5 μg of nuclear extracts from MCF7 cells, and subclones were prepared as previously described (21)

RNA isolation and reverse transcription-PCR analyses

RNA was isolated from MCF7 cells and its subclones using the RNeasy kit and reverse transcribed using the Omniscript RT kit (Qiagen) according to the manufacturer's instructions. The amplification primers for CXCL14 were 5′-GTCCAAATGCAAGTGCTCCC-3′ (forward) and 5′-TTCTTCGTAGACCCTGCGCT-3′ (reverse), and for β-actin were 5′-GCATCGTCACCAACTGGGAC-3′ (forward) and 5′-ACCTGGCCGTCAGGCAGCTC-3′ (reverse). cDNA was amplified using standard PCR conditions.

Subcellular fractionation and microsome Ca^{2+} release assay

Mitochondria and ER were isolated from cells as previously described (22). Microsomes from MCF7 cells were isolated using an Endoplasmic Reticulum Isolation kit according to the manufacturer's instructions (Sigma) and used immediately to assay Ca^{2+} release as described by Guillemette and colleagues (23).

Measurement of Ca^{2+} influx in whole cells

Cells were loaded for 1 h with 5 μmol/L Fluo-3-AM (1×10^6 cells/mL) in Ca^{2+}-free HBSS buffer containing 1% bovine serum albumin. Then, cells were washed twice with HBSS and resuspended in HBSS containing 2 mmol/L Ca^{2+}. Ca^{2+} influx was measured by flow cytometry and triggered by the addition of 2 μmol/L thapsigargin after 10 s. To ensure proper loading, Ca^{2+} influx from each cell line was stimulated with 2 μmol/L ionomycin. Analysis was done using a FACScan flow cytometer (Becton Dickinson), and the kinetic analysis of Fluo-3 versus time as the mean value of individual cells was done using FlowJo software (Tree Star, Inc.).

Animal studies

Six-week-old female BABL/c nude mice were inoculated on the mammary fat pads with MCF7 or its subclones. In both cases, 2×10^6 cells were combined with 100 μL of DMEM-F12 and Matrigel (1:1; BD Biosciences). Mice were inspected daily, and their well-being and body weight monitored. Moribund animals were euthanized as mandated by the Institutional Animal

NIH-PA Author Manuscript

NIH-PA Author Manuscript

NIH-PA Author Manuscript

Care and Use Committee (IACUC) protocol, and the time of death was recorded. Tumor tissues from representative mice were sectioned, embedded in paraffin, and stained with H&E for histopathologic evaluation.

Statistical analysis

Student's *t* test was used to evaluate the statistical differences between the experimental values of two samples being compared. $P < 0.05$ was considered statistically significant.

Results

Generation and characterization of MCF7 subclones with aggressive cellular behaviors

To study the role of mitochondrial dysfunction in invasion, we developed an experimental system using human breast cancer MCF7 cells, which can form localized tumors in nude mice with estrogen supplement but are weakly metastatic. Because electron leakage from the mitochondrial respiratory chain is a major source of ROS, we hypothesized that a disruption of mitochondrial respiration would increase ROS, which may promote genetic instability and the emergence of more aggressive malignant cells. As illustrated in Fig. 1*A*, we used rotenone, an inhibitor of the electron transport complex I known to promote superoxide generation (18), to induce ROS stress in MCF7 cells. After three cycles of rotenone treatment, the cells were plated in drug-free medium to allow the formation of colonies. Among 16 clones picked, two clones (H and P) with high ROS and active cell migration were selected for further studies. Figure 1*B* shows the representative ROS levels. Interestingly, the increased ROS in these clones persisted for at least 6 months without rotenone, likely reflecting persistent mitochondrial dysfunction. In fact, both H and P clones still exhibited reduced mitochondrial respiration, as indicated by a decrease in oxygen consumption (Fig. 1*C*) and a compensatory increase in glycolysis, as indicated by higher glucose uptake and lactate production (Fig. 1*C*). Analysis of cellular ATP showed that both clones had similar cellular ATP compared with the parental MCF7 cells (Supplementary Fig. S1), suggesting that the up-regulation of glycolysis was sufficient to compensate the decreased ATP generation in the mitochondria. Consistently, the subclones exhibited a slight increase in their mitochondrial mass with similar transmembrane potential (Fig. 1*D*). The subclones showed similar or slightly higher proliferation (Fig. 1*D*, *right*). These results are consistent with the previous observations that increased mitochondrial mass and mtDNA contents are early molecular events in response to endogenous oxidative stress (24).

Because ROS can alter gene expression (10,25) and stimulate cell invasiveness (26), we tested the motility and invasive potential of the subclones. A wound healing assay showed that H and P clones exhibited a higher capacity to migrate and fill the gap in culture compared with MCF7 (Fig. 2*A*). To evaluate whether the increase in ROS in H and P clones was essential for this process, cells were pretreated with the antioxidant *N*-acetyl cysteine (NAC) before the wound healing assay. NAC effectively inhibited cell motility (Fig. 2*A*). We also isolated several clones from MCF7 cells without treatment with rotenone as control. No significant change in motility was observed (Supplementary Fig. S2). Subclones H and P exhibited significantly greater ability than the parental MCF7 cells to migrate through a layer of matrix gel and pass membrane pores (Fig. 2*B* and *C*). Furthermore, colony formation assay in soft agar showed similar or slightly higher anchorage-independent colony-forming rates (number of colonies per well) in the subclones, but the size of each colony was smaller than those of MCF7 cells (Supplementary Fig. S3).

We then tested the ability of clones P and H and the parental MCF7 cells to form tumors *in vivo*. Parental MCF7 cells and P and H clones were inoculated on the mammary fat pads of 6-week-old BABL/c nude mice. Both the P and H clones formed palpable tumors in the absence

NIH-PA Author Manuscript

NIH-PA Author Manuscript

NIH-PA Author Manuscript

of exogenous estrogen, whereas the parental MCF7 cells exhibited poor ability to form tumors under these conditions. Three of the five mice inoculated with P clone cells exhibited extensive metastasis to liver, lung, and spleen. The histologic morphology of the primary and metastatic tumors is shown in Fig. 2*D*. No metastasis was detected in the mice inoculated with H clone cells by the time when the primary tumor reached the maximal size requiring euthanasia, as mandated by the IACUC-approved protocol. No metastasis was observed in mice inoculated with the parental MCF7 cells.

ROS promotes CXCL14 expression in MCF7 subclone cells through activation of AP-1

To elucidate the mechanisms by which mitochondrial dysfunction alters cell migration/invasion, we performed microarray analysis of gene expression in several clones of cells with increased ROS. We observed that the expression of CXCL14, a novel chemokine, was significantly elevated in all clones tested in comparison with MCF7 cells. The overexpression of CXCL14 in clones P and H was confirmed by reverse transcription-PCR (RT-PCR) and Western blotting (Fig. 3*A*). The ability of CXCL14 to stimulate cell migration was then tested using the wound healing assay. Figure 3*B* shows that recombinant CXCL14 protein (0.57 ng/mL) significantly enhanced MCF7 cell migration. Furthermore, conditioned medium from clones P and H also promoted cell migration (Fig. 3*B*). Ectopic overexpression of *CXCL14* in MCF7 cells by transfection also rendered the cells highly migratory (Fig. 3*C*). To further evaluate the relationship between the induction of CXCL14 and increased migration and invasion, we used a decoy strategy using a synthetic double-stranded phosphorothioate oligonucleotide, which contained a hairpin structure resembling the *CXCL14* promoter region and functioned as a *cis*-element to suppress *CXCL14* expression. Transfection of H clone with the decoy DNA efficiently suppressed CXCL14 transcription and inhibited cellular migration, as evidenced by the reduced numbers of cells migrating through the membrane (Fig. 3*D*).

We then used an antioxidant to investigate whether ROS regulate *CXCL14* expression. NAC partially suppressed the expression of CXCL14 in clone P (Fig. 4*A*, *bottom*) and clone H (data not shown), suggesting that CXCL14 expression might be regulated by ROS. Consistently, hydrogen peroxide (H_2O_2) promoted *CXCL14* expression in a time- and dose-dependent manner (Fig. 4*A*, *top*). Interestingly, another clone with slower proliferation rate (clone D) also exhibited increase ROS generation, higher *CXCL14* expression, and active cell motility (Supplementary Fig. S4). Thus, the increase in cell motility was correlated with ROS generation and *CXCL14* expression and was not due to active proliferation.

To further explore the mechanism by which ROS regulate *CXCL14* expression, we performed a gene database analysis and identified a potential AP-1 binding sequence within the putative promoter region of *CXCL14*. EMSA assay using a radioactively labeled oligonucleotide containing the AP-1 consensus sequence showed that both subclones (H and P) had an increase in AP-1 activity compared with the parental cells (Fig. 4*B*, *left*). Furthermore, nuclear extract from MCF7 cells exposed to H_2O_2 for 20 minutes showed a significant increase in AP-1 DNA binding (Fig. 4*B*, *right*), suggesting a role of ROS in regulating CXCL14 expression through AP-1. To test this possibility, the CXCL14-overexpressing cells (clone H) were incubated with the c-Jun-NH_2-kinase (JNK) inhibitor SP600125 to block c-Jun (a component of AP-1) activation and then tested if this would cause a decrease of CXCL14 transcription. Indeed, SP600125 inhibited AP-1 DNA binding and reduced CXCL14 expression at the mRNA and protein levels (Fig. 4*C*). Chromatin immunoprecipitation was then used to analyze if AP-1 binds to *CXCL14* promoter. As shown in Fig. 4*D*, after protein-DNA cross-linking, immunoprecipitation with AP-1 antibody pulled down the *CXCL14* promoter DNA sequence, which was detected by PCR using specific primers spanning the −323 to −83 region of the human *CXCL14* promoter. These results show that AP-1 binds to *CXCL14* promoter.

NIH-PA Author Manuscript

NIH-PA Author Manuscript

NIH-PA Author Manuscript

CXCL14 induced an increase in cellular Ca^{2+} through interaction with IP_3R

Because Ca^{2+} plays an essential role in cell motility and the ER is a major regulator of cellular Ca^{2+} homeostasis (27), we tested if CXCL14 affects ER function and alters cytosolic Ca^{2+} in the subclones. Using subcellular fractionations, we found that CXCL14 was significantly higher in the ER compartments of clones H and P than MCF7 cells (Fig. 5*A*). Interestingly, analysis of cytosolic Ca^{2+} revealed that clones H and P had significantly higher cytosolic Ca^{2+} contents than the parental MCF7 cells (Fig. 5*B*, *left*), whereas the ER Ca^{2+} levels were significantly lower in clones H and P (Fig. 5B, *right*). This suggests a possible "leakage" of Ca^{2+} from the ER to the cytosol associated with the localization of CXCL14 to ER. Transfection of MCF7 cells with *CXCL14* caused an increase in cytosolic Ca^{2+} (Fig. 5*C*). Because the IP_3R of ER plays an important role in Ca^{2+} signaling via interaction with inositol 1,4,5-trisphosphate (IP_3; ref. 28), we examined whether CXCL14 binds to IP_3R and disturbs its function. Immunoprecipitation with IP_3R antibody and Western blotting of the pulled-down products using anti-CXCL14 showed a physical association between CXCL14 and IP_3R (Fig. 5*D*). We reasoned that if the binding of CXCL14 to IP_3R caused a leak of Ca^{2+} from the ER to the cytosol, the amount of Ca^{2+} stored in the ER would be lower in the subclones than in the parental MCF7 cells and that a release of ER Ca^{2+} into the cytosol triggered by thapsigargin would cause less increase of cytosolic Ca^{2+} in the subclones. As shown in Fig. 6*A*, thapsigargin caused a rapid increase of cytosolic Ca^{2+} in MCF7 cells and a substantially smaller Ca^{2+} increase in the P clone cells, suggesting lower ER Ca^{2+} storage in P cells. The effect of thapsigargin on Ca^{2+} levels in these cells was further investigated in the presence of 100 μmol/L 2-aminoethoxydiphenyl borate (2-APB), a compound that blocks receptor-induced Ca^{2+} store emptying (29). Preincubation of MCF7 cells with 2-APB almost completely suppressed thapsigargin-induced Ca^{2+} release in MCF7 cells, but this effect was substantially attenuated in clone P (Fig. 6*A*). Thus, CXCL14 might interact with the 2-APB–sensitive domain of IP_3R, leading to Ca^{2+} leakage and a blunted response to thapsigargin.

To directly test the role of CXCL14 on Ca^{2+} flux regulation in the ER, we isolated the ER fraction from MCF7 cells and measured Ca^{2+} release from the ER microsomes in the presence and absence of purified CXCL14 protein. As shown in Fig. 6*B* to *D*, CXCL14 induced Ca^{2+} release from the ER microsomes in a time- and dose-dependent manner. As a positive control, Ca^{2+} release was triggered by 10 μmol/L IP_3 to activate IP_3R or by 10 μmol/L thapsigargin to inhibit the ER Ca^{2+} pump. As expected, IP_3 and thapsigargin caused a dramatic Ca^{2+} release, whereas CXCL14 induced a moderate but consistent Ca^{2+} release (Fig. 6*D*). This may explain why overexpression of CXCL14 led to a moderate and sustained increase in cytosolic Ca^{2+} without causing cytotoxicity.

Discussion

Breast cancer metastasis represents a major challenge in clinical treatment of this disease, and the detailed mechanisms that regulate breast cancer cell motility and metastasis remain to be an important research area. It is known that mitochondria are major sites of ROS generation in the cells and that ROS can function as signaling molecules to stimulate cell proliferation and promote cell motility (1). Interestingly, mitochondria dysfunction has been shown to contribute to tumor progression by enhancing the metastatic potential of tumor cells (30). However, the mechanism by which ROS stimulates cell motility is still unclear. The present study provides several lines of evidence suggesting that increased expression of CXCL14 may play an important role in this process. (*a*) Both clones H and P, which were isolated after chemical disruption of the mitochondrial respiration in MCF7 cells, exhibit increased ROS, cellular motility, and ability to invade through Matrigel. These malignant behaviors were suppressed by the antioxidant NAC, indicating the important role of ROS, which was associated with mitochondrial dysfunction. (*b*) CXCL14 was overexpressed in both H and P

NIH-PA Author Manuscript

NIH-PA Author Manuscript

NIH-PA Author Manuscript

clones, and this expression was stimulated by exogenous ROS and suppressed by NAC. (*c*) The role of CXCL14 in promoting cell migration and invasion was shown by direct stimulation of cell motility using recombinant CXCL14 protein, conditional medium, or overexpression of CXCL14 through gene transfection. (*d*) CXCL14 caused Ca^{2+} leakage from the ER through binding to IP_3R, leading to increased cytosolic Ca^{2+}. (*e*) ROS seem to induce CXCL14 expression through activation of the AP-1 pathway, as shown by specific decoy DNA, JNK inhibitor, and antioxidant.

CXCL14 (also known as BRAK or MIP-2γ) is a chemokine with yet unknown function (31, 32). This molecule was first identified by differential display using normal epithelial cells and head and neck squamous carcinoma cells and was shown to be expressed in normal epithelial tissues and in various tumors of epithelial origin with heterogeneous expression levels (31, 33). The receptor for CXCL14 has not yet been identified, and conflicting biological functions of this molecule are described in the literature (34–37). CXCL14 is associated with the development and progression of breast cancer, and its gene expression level is correlated with the clinical metastases time of breast cancer patients (38). Moreover, CXCL14 seems to increase the invasiveness of pancreatic cancer cells by activation of the nuclear factor-κB pathway (39). Our study suggests that in breast cancer cells, CXCL14 promotes cell motility through its ability to induce release of Ca^{2+} to the cytosol.

CXCL14 seems to provide a molecular link between ROS stress and increased cell motility. DNA analysis revealed that the CXCL14 putative promoter region contains a binding site for AP-1, a transcription regulatory complex known to be redox sensitive. We showed that inhibition of JNK by SP600125 suppressed AP-1 DNA binding activity and reduced CXCL14 expression. The AP-1 decoy also suppressed CXCL14 expression and inhibited cell motility. Thus, activation of AP-1 is a likely mechanism for ROS-induced CXCL14 up-regulation. Interestingly, metastatic breast carcinoma cells (estrogen receptor negative) have higher AP-1 DNA binding activity than do less metastatic carcinomas (estrogen receptor positive), and expression of Fra-1 correlates with AP-1 activity and invasiveness in these cells (40). Several AP-1–responsive genes with roles in facilitating the invasion of malignant cells have been described (41,42), and our study suggests that CXCL14 is another important AP-1 effector. Our observations that mitochondrial dysfunction induces ROS-mediated AP-1 activation and CXCL14 up-regulation is consistent with a recent study that mitochondrial oxidative stress through overproduction of H_2O_2 induced the Jun kinase pathway (13).

Calcium plays an essential role in the assembly of actin filaments and cytoskeleton reorganization and, thus, affects cell motility and migration. We found that cytosolic Ca^{2+} levels in both clones H and P were elevated. This increase in cytosolic Ca^{2+} is likely due to the release of Ca^{2+} from the ER. We showed that CXCL14 was present in the ER, physically interacted with IP_3R, and directly induced Ca^{2+} release from isolated ER microsomes. Furthermore, the IP_3R inhibitor 2-APB was significantly less effective in preventing thapsigargin-induced Ca^{2+} mobilization in CXCL14-overexpressing clone P cells than in the parental MCF7 cells. Together, these observations suggest that CXCL14 induces cytosolic Ca^{2+} increase by mobilization of Ca^{2+} from the ER through binding to IP_3R, and that CXCL14 might attenuate the function of 2-APB–sensitive IP_3R channels. In future study, it would be interesting to further determine the detailed molecular interaction between CXCL14 and IP_3R through systemic deletion of the CXCL14 peptide segments to identify the interface responsible for binding, and use specific antibodies to show the colocalization of the two molecules on the ER membranes.

Although a high level of cytosolic Ca^{2+} can stimulate mitochondrial respiration in cells with competent mitochondrial, this may not happen in cells with compromised mitochondrial function. In our experimental system, the Ca^{2+} increase seemed to be a consequence of

NIH-PA Author Manuscript

NIH-PA Author Manuscript

NIH-PA Author Manuscript

mitochondria dysfunction initially induced by rotenone. It is unclear if the increased cytosolic Ca^{2+} may play a role in up-regulation of glycolysis. Interestingly, most glycolytic enzymes bind to cytoskeleton, and it is possible that increased cytosolic Ca^{2+} might promote the assembly of cytoskeleton-bound glycolytic enzymes leading to high glycolytic activity.

Of note, the aggressive malignant cell behaviors of the clones H and P were stable after the cells were cultured in medium free of rotenone, suggesting a possibility that the initial ROS increase induced by rotenone might have induced mutations in mtDNA or/and nuclear DNA. We have attempted to identify mtDNA mutations by direct sequencing of mtDNA for these two subclones in comparison with the parental MCF7 cells. No mtDNA mutation was detected. It is possible that in clones H and P, mutation(s) might have occurred in the nuclear DNA at a gene that affects mitochondrial function leading to decreased respiration and increased glycolysis, which seemed to affect cell proliferation and colony formation in a complex manner: high colony number but smaller colony sizes. Although the exact reason for such complex growth alterations remain unclear, this phenomenon may explain why the subclones showed similar overall cell growth curves compared with the parental MCF7 cells, as measured by direct counting of cell number (Fig. 1*D*, *right*).

In conclusion, our findings suggest that mitochondrial dysfunction in human breast cancer cells can promote cell motility and invasive behaviors through the AP-1/CXCL14/calcium pathway. The increased ROS in cancer may promote cellular proliferation and migration leading to more aggressive malignant behaviors and metastasis. It should be pointed out, however, that because elevated ROS may also cause cellular damage and induce senescence, only those cancer cells capable of mobilizing their antioxidant systems and other regulatory mechanisms to effectively counteract the adverse effects of ROS can reestablish redox balance and emerge as highly malignant clones. In fact, we observed that the cancer cells with high ROS generation in long-term culture tended to rebalance their ROS generation and elimination, leading to a steady redox state that favored their continuous proliferation in culture. Thus, ROS signaling and its roles in cancer development and metastasis are extremely complex biological processes. Understanding these mechanisms is essential for developing new therapeutic strategies to effectively inhibit cancer growth and prevent metastasis.

Supplementary Material

Refer to Web version on PubMed Central for supplementary material.

Acknowledgments

Grant support: National Cancer Institute grants CA85563, CA109041, CA100428, CA100632, and CA16672.

We thank Wendy D. Schober and K. Dwyer for flow cytometry analysis and Kenneth Dunner, Jr. for assistance in the transmission electron microscopy studies.

References

1. Storz P. Reactive oxygen species in tumor progression. Front Biosci 2005;10:1881–1896. [PubMed: 15769673]
2. Radisky DC, Levy DD, Littlepage LE, et al. Rac1b and reactive oxygen species mediate MMP-3-induced EMT and genomic instability. Nature 2005;436:123–127. [PubMed: 16001073]
3. Ristow M. Oxidative metabolism in cancer growth. Curr Opin Clin Nutr Metab Care 2006;9:339–345. [PubMed: 16778561]
4. Wu M, Neilson A, Swift AL, et al. Multiparameter metabolic analysis reveals a close link between attenuated mitochondrial bioenergetic function and enhanced glycolysis dependency in human tumor cells. Am J Physiol Cell Physiol 2007;292:C125–C136. [PubMed: 16971499]

NIH-PA Author Manuscript

NIH-PA Author Manuscript

NIH-PA Author Manuscript

5. Pelicano H, Carney D, Huang P. ROS stress in cancer cells and therapeutic implications. Drug Resist Updat 2004;7:97–110. [PubMed: 15158766]
6. Pelicano H, Martin DS, Xu RH, Huang P. Glycolysis inhibition for anticancer treatment. Oncogene 2006;25:4633–4646. [PubMed: 16892078]
7. Moreno-Sanchez R, Rodriguez-Enriquez S, Marin-Hernandez A, Saavedra E. Energy metabolism in tumor cells. FEBS J 2007;274:1393–1418. [PubMed: 17302740]
8. Suh YA, Arnold RS, Lassegue B, et al. Cell transformation by the superoxide-generating oxidase Mox1. Nature 1999;401:79–82. [PubMed: 10485709]
9. Huang P, Feng L, Oldham EA, Keating MJ, Plunkett W. Superoxide dismutase as a target for the selective killing of cancer cells. Nature 2000;407:309–311. [PubMed: 11014172]
10. Droge W. Free radicals in the physiological control of cell function. Physiol Rev 2002;82:47–95. [PubMed: 11773609]
11. Klaunig JE, Kamendulis LM. The role of oxidative stress in carcinogenesis. Annu Rev Pharmacol Toxicol 2004;44:239–267. [PubMed: 14744246]
12. Hanahan D, Weinberg RA. The hallmarks of cancer. Cell 2000;100:57–70. [PubMed: 10647931]
13. Nemoto S, Takeda K, Yu ZX, Ferrans VJ, Finkel T. Role for mitochondrial oxidants as regulators of cellular metabolism. Mol Cell Biol 2000;20:7311–7318. [PubMed: 10982848]
14. Samper E, Nicholls DG, Melov S. Mitochondrial oxidative stress causes chromosomal instability of mouse embryonic fibroblasts. Aging Cell 2003;2:277–285. [PubMed: 14570235]
15. Warburg O. On the origin of cancer cells. Science 1956;123:309–314. [PubMed: 13298683]
16. Alirol E, Martinou JC. Mitochondria and cancer: is there a morphological connection? Oncogene 2006;25:4706–4716. [PubMed: 16892084]
17. Chatterjee A, Mambo E, Sidransky D. Mitochondrial DNA mutations in human cancer. Oncogene 2006;25:4663–4674. [PubMed: 16892080]
18. Pelicano H, Feng L, Zhou Y, et al. Inhibition of mitochondrial respiration: a novel strategy to enhance drug-induced apoptosis in human leukemia cells by a reactive oxygen species-mediated mechanism. J Biol Chem 2003;278:37832–37839. [PubMed: 12853461]
19. Xu RH, Pelicano H, Zhou Y, et al. Inhibition of glycolysis in cancer cells: a novel strategy to overcome drug resistance associated with mitochondrial respiratory defect and hypoxia. Cancer Res 2005;65:613–621. [PubMed: 15695406]
20. Robinson, JP.; Darzynkiewicz, Z.; Dean, PN., et al. Current protocols in cytometry. New York: John Wiley & Sons, Inc.; 2000.
21. Pines A, Perrone L, Bivi N, et al. Activation of APE1/Ref-1 is dependent on reactive oxygen species generated after purinergic receptor stimulation by ATP. Nucleic Acids Res 2005;33:4379–4394. [PubMed: 16077024]
22. Morimoto, T.; Sabatini, DD.; Doda, JN. Subcellular fractionation. In: Spector, DL.; Goldman, RD.; Leinwand, LA., editors. Cells: a laboratory manual, culture of cells and biochemical analysis. New York: Cold Spring Harbor Laboratory; 1998. p. 34.1-41.4.
23. Guillemette G, Balla T, Baukal AJ, Catt KJ. Characterization of inositol 1,4,5-trisphosphate receptors and calcium mobilization in a hepatic plasma membrane fraction. J Biol Chem 1988;263:4541–4548. [PubMed: 2832398]
24. Lee HC, Yin PH, Lu CY, Chi CW, Wei YH. Increase of mitochondria and mitochondrial DNA in response to oxidative stress in human cells. Biochem J 2000;348:425–432. [PubMed: 10816438]
25. Finkel T. Oxidant signals and oxidative stress. Curr Opin Cell Biol 2003;15:247–254. [PubMed: 12648682]
26. Mori K, Shibanuma M, Nose K. Invasive potential induced under long-term oxidative stress in mammary epithelial cells. Cancer Res 2004;64:7464–7472. [PubMed: 15492271]
27. Berridge MJ, Bootman MD, Roderick HL. Calcium signalling: dynamics, homeostasis and remodelling. Nat Rev Mol Cell Biol 2003;4:517–529. [PubMed: 12838335]
28. Berridge MJ. Elementary and global aspects of calcium signalling. J Physiol 1997;499:291–306. [PubMed: 9080360]

NIH-PA Author Manuscript

NIH-PA Author Manuscript

NIH-PA Author Manuscript

29. Maruyama T, Kanaji T, Nakade S, Kanno T, Mikoshiba K. 2APB, 2-aminoethoxydiphenyl borate, a membrane-penetrable modulator of Ins(1,4,5)P3-induced Ca^{2+} release. J Biochem (Tokyo) 1997;122:498–505. [PubMed: 9348075]
30. Ishikawa K, Takenaga K, Akimoto M, et al. ROS-generating mitochondrial DNA mutations can regulate tumor cell metastasis. Science 2008;320:661–664. [PubMed: 18388260]
31. Frederick MJ, Henderson Y, Xu X, et al. *In vivo* expression of the novel CXC chemokine BRAK in normal and cancerous human tissue. Am J Pathol 2000;156:1937–1950. [PubMed: 10854217]
32. Hromas R, Broxmeyer HE, Kim C, et al. Cloning of BRAK, a novel divergent CXC chemokine preferentially expressed in normal versus malignant cells. Biochem Biophys Res Commun 1999;255:703–706. [PubMed: 10049774]
33. Schwarze SR, Luo J, Isaacs WB, Jarrard DF. Modulation of CXCL14 (BRAK) expression in prostate cancer. Prostate 2005;64:67–74. [PubMed: 15651028]
34. Kurth I, Willimann K, Schaerli P, Hunziker T, Clark-Lewis I, Moser B. Monocyte selectivity and tissue localization suggests a role for breast and kidney-expressed chemokine (BRAK) in macrophage development. J Exp Med 2001;194:855–861. [PubMed: 11561000]
35. Shellenberger TD, Wang M, Gujrati M, et al. BRAK/CXCL14 is a potent inhibitor of angiogenesis and is a chemotactic factor for immature dendritic cells. Cancer Res 2004;64:8262–8270. [PubMed: 15548693]
36. Shurin GV, Ferris RL, Tourkova IL, et al. Loss of new chemokine CXCL14 in tumor tissue is associated with low infiltration by dendritic cells (DC), while restoration of human CXCL14 expression in tumor cells causes attraction of DC both *in vitro* and *in vivo*. J Immunol 2005;174:5490–5498. [PubMed: 15843547]
37. Allinen M, Beroukhim R, Cai L, et al. Molecular characterization of the tumor microenvironment in breast cancer. Cancer Cell 2004;6:17–32. [PubMed: 15261139]
38. Chiu SH, Chen CC, Lin TH. Using support vector regression to model the correlation between the clinical metastases time and gene expression profile for breast cancer. Artif Intell Med 2008;44:221–231. [PubMed: 18678474]
39. Wente MN, Mayer C, Gaida MM, et al. CXCL14 expression and potential function in pancreatic cancer. Cancer Lett 2008;259:209–217. [PubMed: 18054154]
40. Philips A, Teyssier C, Galtier F, et al. FRA-1 expression level modulates regulation of activator protein-1 activity by estradiol in breast cancer cells. Mol Endocrinol 1998;12:973–985. [PubMed: 9658402]
41. Crowe DL, Tsang KJ, Shemirani B. Jun N-terminal kinase 1 mediates transcriptional induction of matrix metalloproteinase 9 expression. Neoplasia 2001;3:27–32. [PubMed: 11326313]
42. Vleugel MM, Greijer E, Bos R, van der Wall E, van Diest PJ. c-Jun activation is associated with proliferation and angiogenesis in invasive breast cancer. Hum Pathol 2006;37:668–674. [PubMed: 16733206]

NIH-PA Author Manuscript
NIH-PA Author Manuscript
NIH-PA Author Manuscript

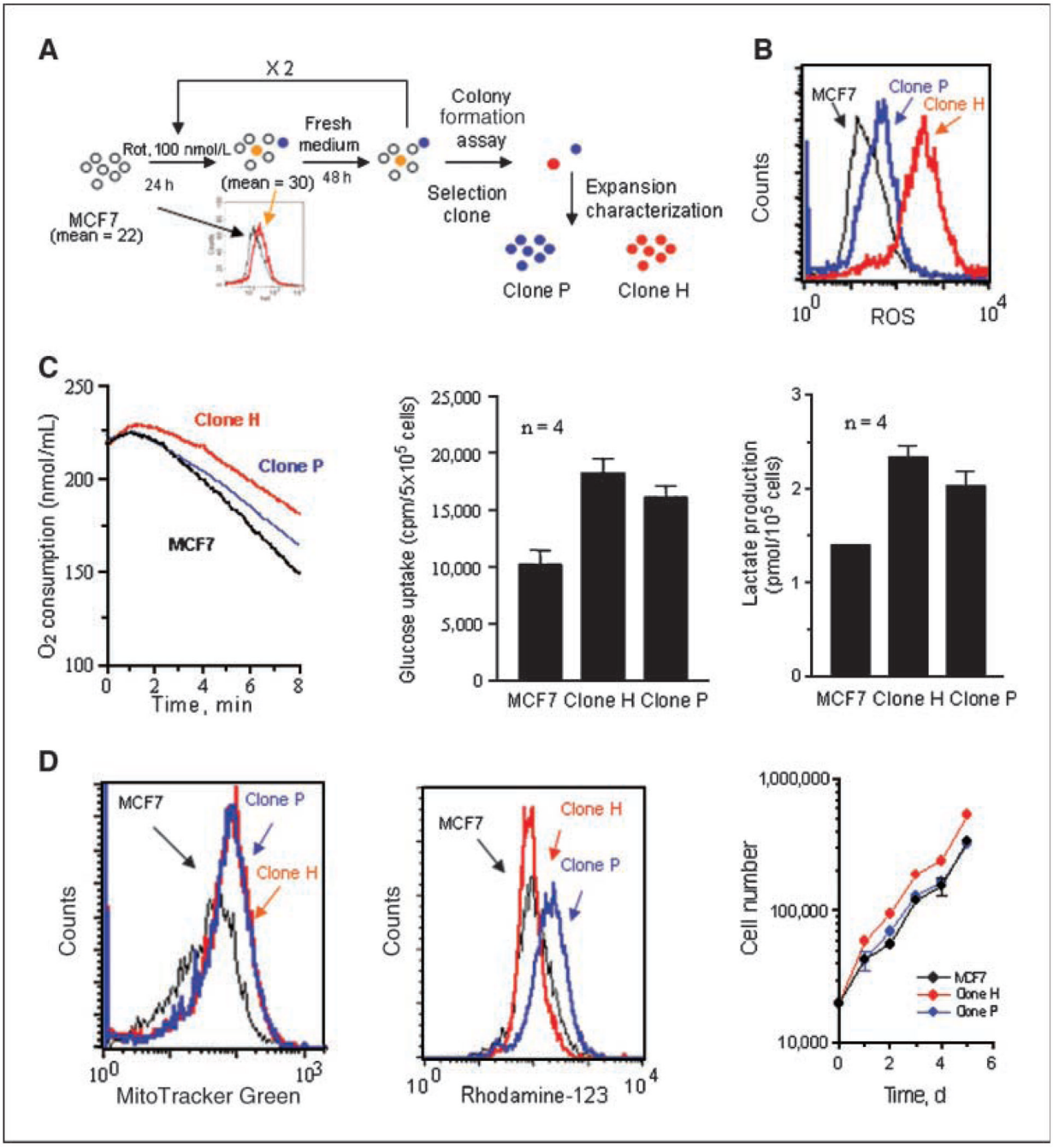

Figure 1.

Biochemical characterization of mitochondria dysfunction of H and P clone cells. *A*, schematic representation of the establishment of MCF7 subclones. Cells were treated for 24 h with rotenone (100 nmol/L), which caused an increase in superoxide generation, as measured by flow cytometry (*left* ; numbers indicate the mean superoxide values). Cells were then cultured in drug-free medium for 48 h, followed by two more cycles of rotenone treatment. Cells were then plated at a density of 200 per dish and colonies were isolated. *B*, comparison of ROS generation by parental MCF7 cells and its subclones (H and P clones) using 3 μmol/L CM-H_2DCF-DA measured by flow cytometry. *C*, comparison of oxygen consumption (*left*), glucose uptake (*center*), and lactate production (*right*) in MCF7 cells and subclones.

Columns, mean of three independent experiments; *bars*, SD. *D*, comparison of mitochondrial mass (*left*), mitochondrial transmembrane potential ($\Delta\psi_m$; *center*), and cell growth (*right*) of MCF7 cells and subclones. Results of a representative experiment ($n = 3$).

NIH-PA Author Manuscript
NIH-PA Author Manuscript
NIH-PA Author Manuscript

NIH-PA Author Manuscript
NIH-PA Author Manuscript
NIH-PA Author Manuscript

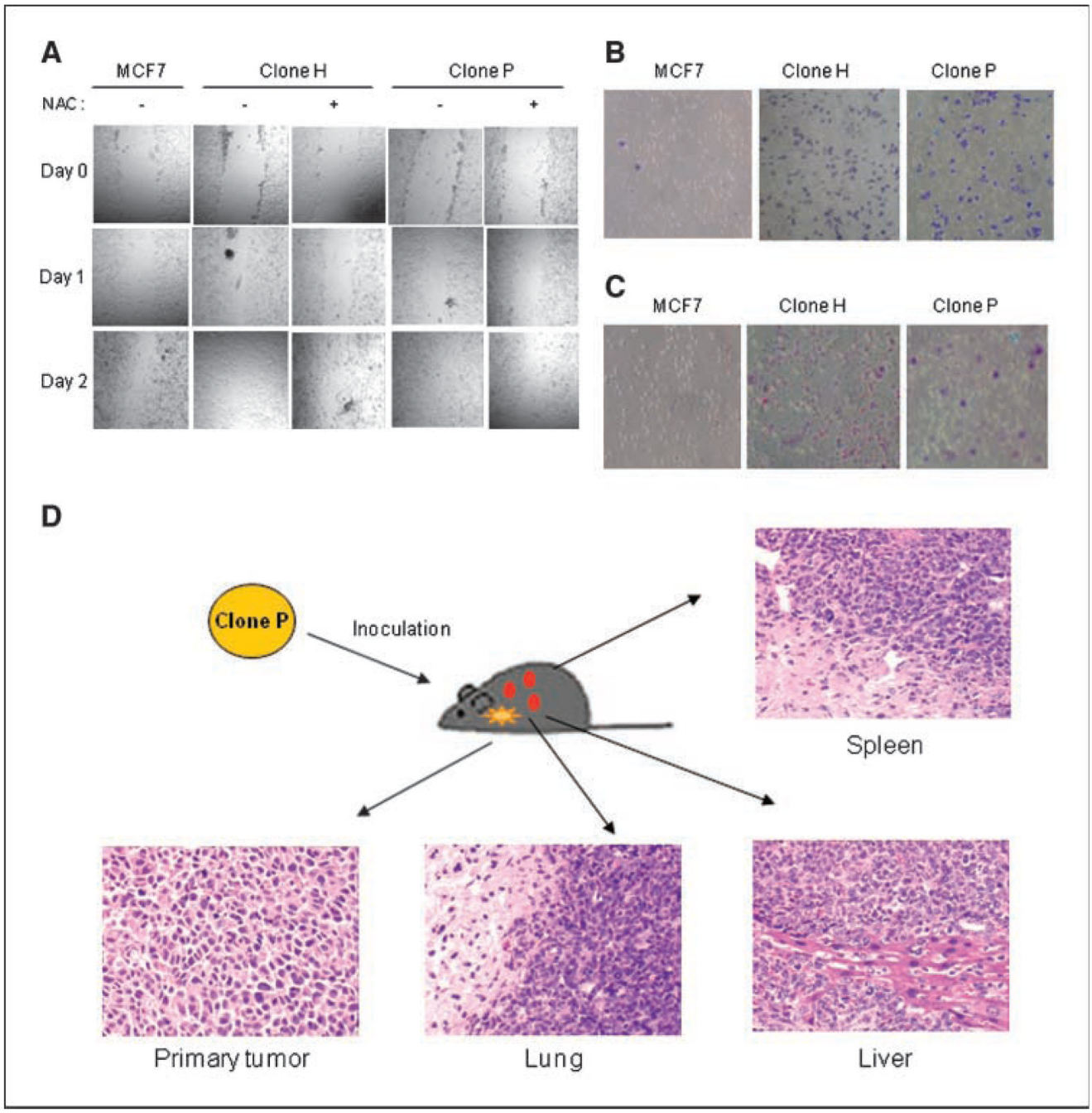

Figure 2.

MCF7 subclones exhibiting mitochondrial dysfunction had more aggressive cellular behaviors than did MCF7 cells. *A*, MCF7 subclones migrated faster than MCF7 cells, as shown in a wound healing assay. The confluent monolayer of cells was pretreated with 5 mmol/L NAC for 3 h (as indicated) and then wounded by scraping a narrow 200-μL pipette tip across the plate. Every day, each well was examined by phase-contrast microscopy for the amount of wound closure, and wound images were captured under a phase-contrast Nikon microscope (Nikon Eclipse TE300). *B*, MCF7 subclones migrated faster than MCF7 cells through uncoated membranes in modified Boyden chamber assays. *C*, MCF7 subclones were more invasive than MCF7 cells. Cells were cultured on transwell cell culture inserts coated with Matrigel. Results

of a representative experiment ($n = 3$). *D*, histologic morphology of H&E-stained tissue slices of clone P tumor and metastasis.

NIH-PA Author Manuscript
NIH-PA Author Manuscript
NIH-PA Author Manuscript

NIH-PA Author Manuscript
NIH-PA Author Manuscript
NIH-PA Author Manuscript

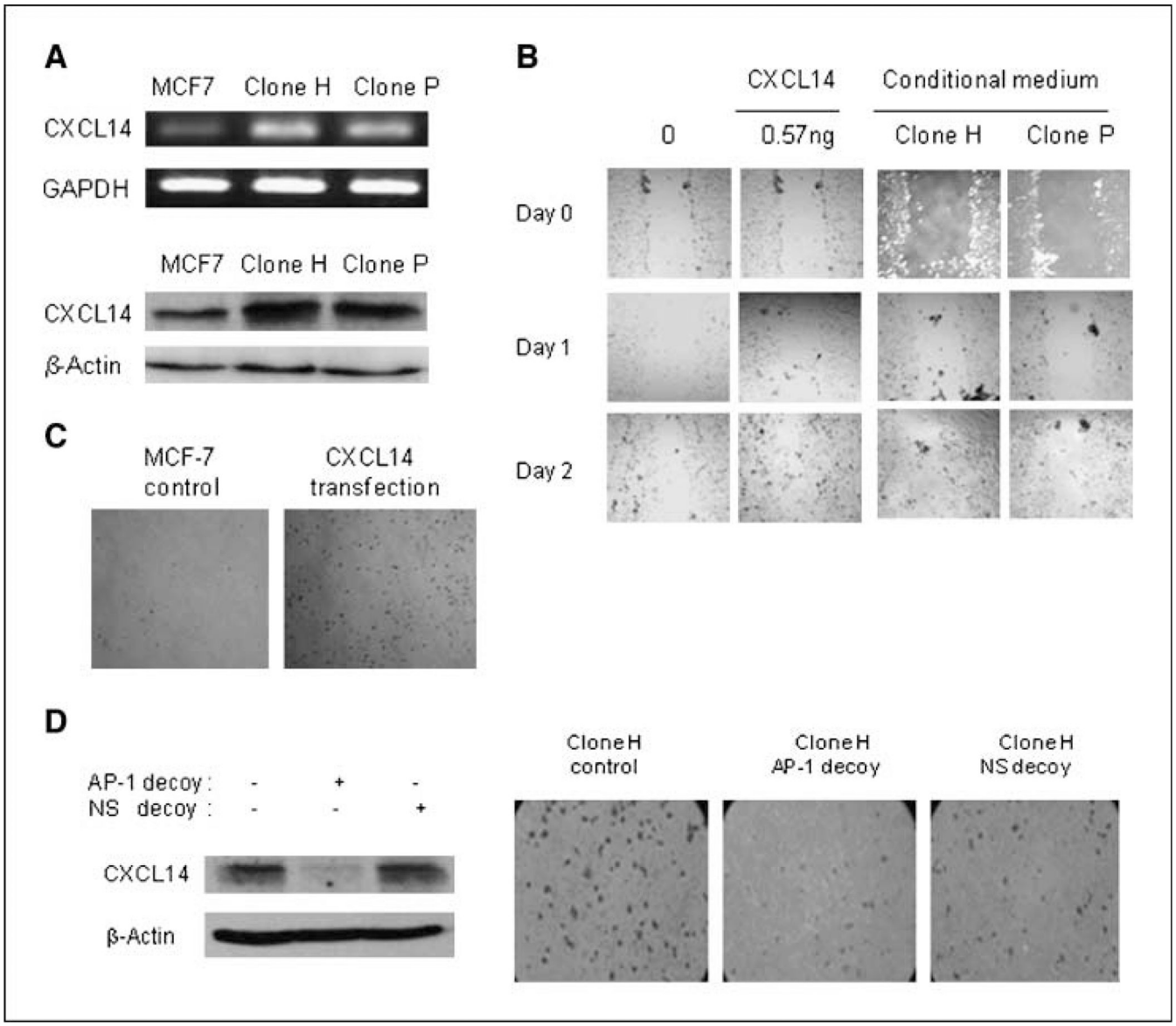

Figure 3.

CXCL14 promotes cell motility. *A*, analysis of CXCL14 expression in MCF7 cells and subclones by RT-PCR (*top*) and by Western blotting (*bottom*). *B*, addition of exogenous CXCL14 promoted MCF7 cell migration *in vitro* . Plated MCF7 cells were grown to confluency, wounded, and then incubated with either 0.57 ng CXCL14 or conditioned medium from H or P clones for 48 h. Each plate was examined by phase-contrast microscopy for the amount of wound closure. *C*, transient transfection of CXCL14 promotes MCF7 cell migration *in vitro* . MCF7 cells were transfected with 0.5 μg of CXCL14 plasmid. After 48 h, cells were collected and used in a migration assay. *D*, inhibition of invasion of clone H by AP-1 decoy. Clone H cells were transfected with either AP-1decoy or scramble decoy (100 pmol). After 48 h, cells were collected and lysed and CXCL14 expression was analyzed by Western blotting (*left*), or cells were collected and cultured on transwell cell culture inserts coated with Matrigel for an additional 20 h (*right*). Results of a representative experiment ($n = 3$).

NIH-PA Author Manuscript
NIH-PA Author Manuscript
NIH-PA Author Manuscript

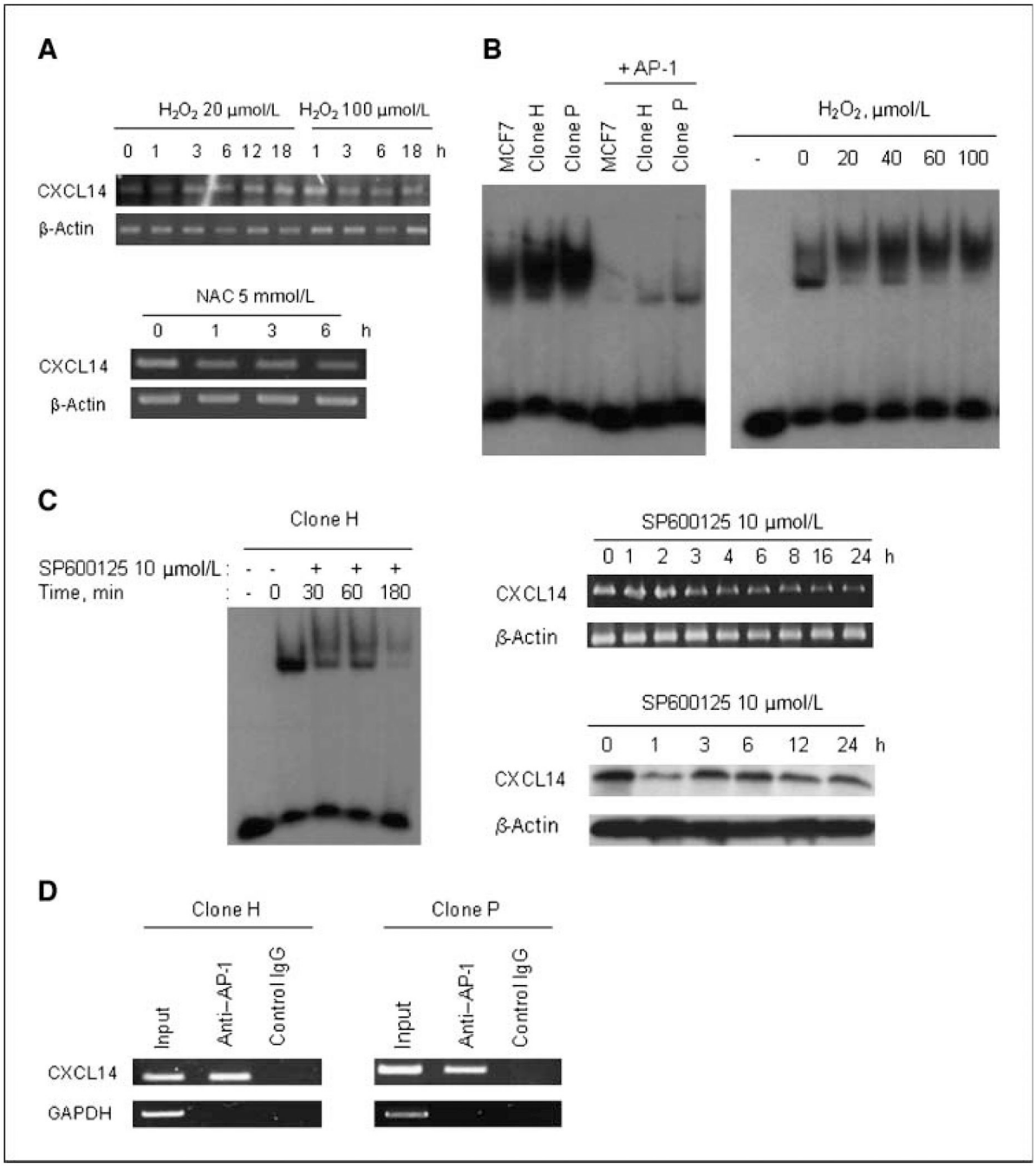

Figure 4.

ROS promotes CXCL14 expression in MCF7 subclone cells through activation of AP-1. *A*, ROS-promoted CXCL14 expression. The induction of CXCL14 mRNA expression by H_2O_2 is time and dose dependent (*top*). MCF7 cells were treated with 20 or 100 μmol/L H_2O_2. RNA was isolated at the indicated time, and CXCL14 mRNA expression was analyzed. NAC down-regulated the mRNA expression of CXCL14 in clone P (*bottom*). Clone P cells were treated with 5 mmol/L NAC. RNA was isolated at the indicated time, and CXCL14 mRNA expression was analyzed. *B*, DNA binding activity of AP-1 in MCF7 cells and its subclones (*left*) and H_2O_2-activated DNA binding activity of AP-1in MCF7 cells (*right*). Nuclear extract from MCF7 cells was prepared and incubated with H_2O_2 at the indicated concentration for 20 min

NIH-PA Author Manuscript

NIH-PA Author Manuscript

NIH-PA Author Manuscript

at 4°C, and then the DNA binding activity of AP-1was determined. *C*, effects of JNK inhibitor on the DNA binding activity of AP-1in MCF7 subclones (*left*). Effects of JNK inhibitor on CXCL14 mRNA expression (*right top*) and protein expression (*right bottom*) in clone H. *D*, detection of the *in vivo* binding of AP-1 protein to the human *CXCL14* promoter in a chromatin immunoprecipitation assay. Results of a representative experiment ($n = 3$).

NIH-PA Author Manuscript

NIH-PA Author Manuscript

NIH-PA Author Manuscript

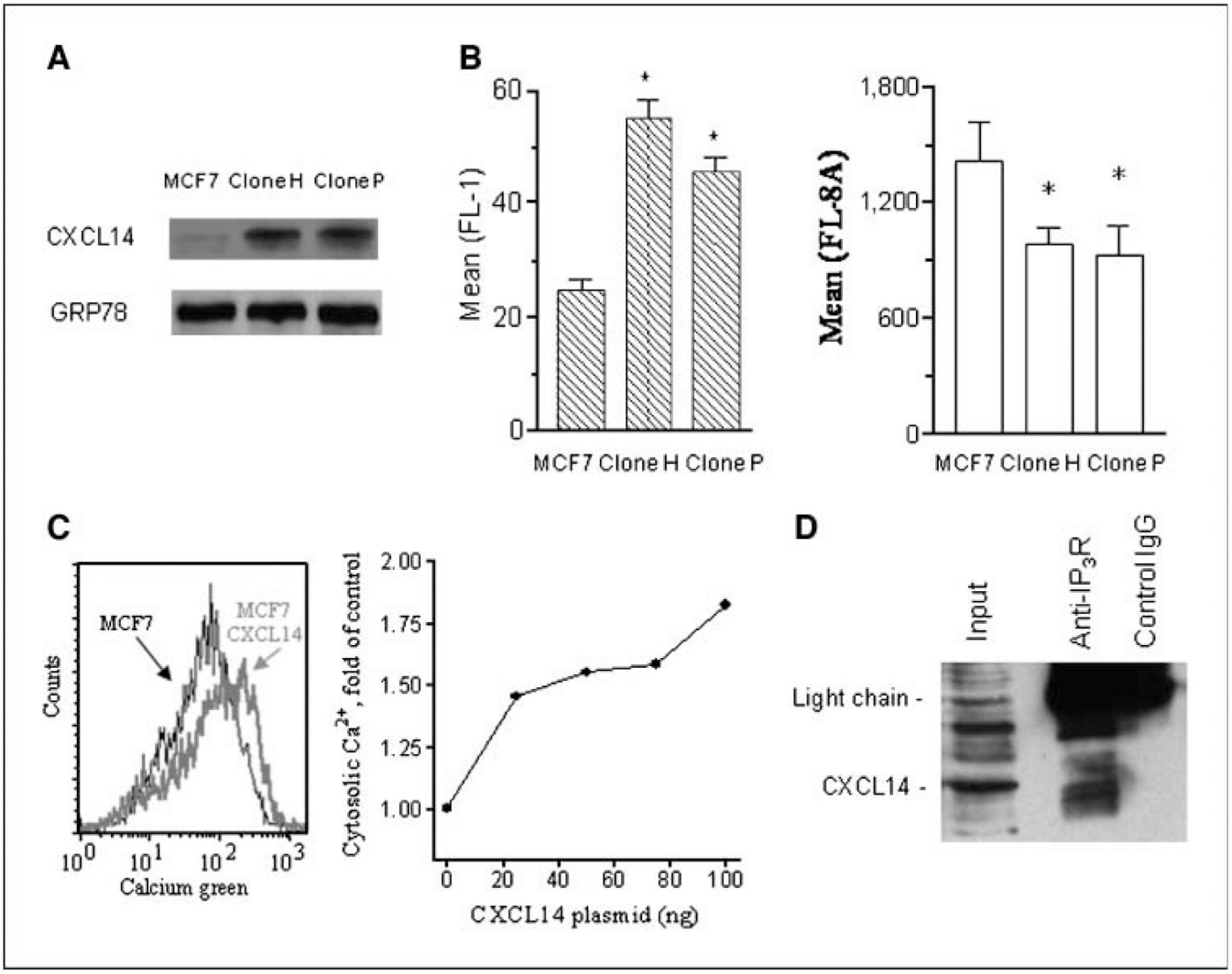

Figure 5.

CXCL14 induced Ca^{2+} release from ER stores through IP_3R. *A*, CXCL14 was localized in the ER. Western blot analysis of CXCL14 from subcellular fractions of MCF7 cells and its subclones. *B*, MCF7 subclones exhibited higher cytosolic Ca^{2+} content, as measured with Calcium Green (*left*). ER Ca^{2+} content was decreased in MCF7 subclones, as measured with ER-Tracker Blue-White DPX (*right*). *, $P < 0.05$, compared with the parental MCF7 cells. *C*, increase of cytosolic Ca^{2+} by CXCL14 (0.75 μg) in MCF7 cells 48 h posttransfection (*left*). The cytosolic Ca^{2+} content increased after CXCL14 transfection in MCF7 in a dose-dependent manner (*right*). *D*, coimmunoprecipitation of CXCL14 with IP_3R. Results of a representative experiment ($n = 3$).

NIH-PA Author Manuscript
NIH-PA Author Manuscript
NIH-PA Author Manuscript

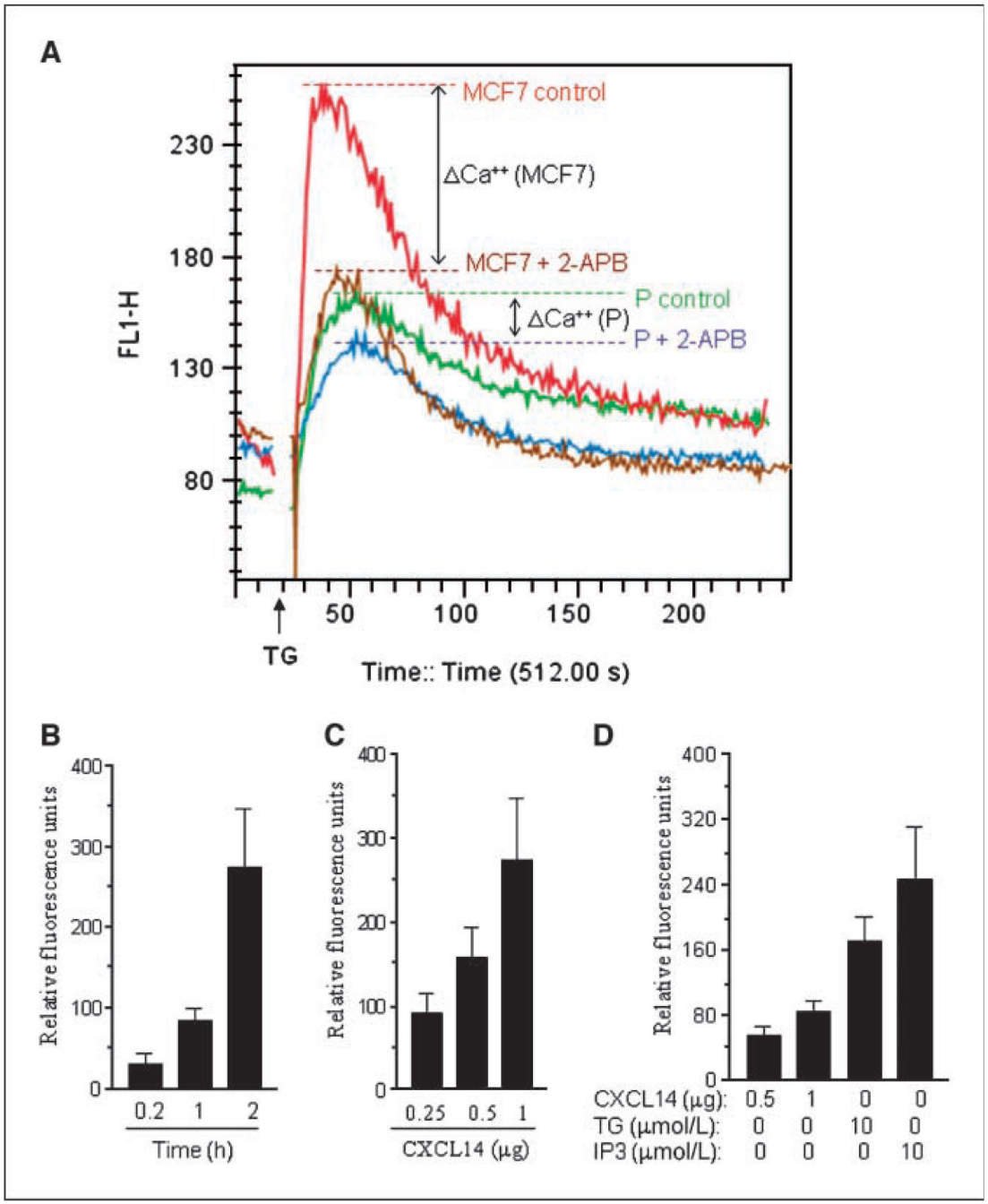

Figure 6.

CXCL14-induced Ca^{2+} release in microsomes and its inhibition by 2-APB in clone P *in vitro*. *A*, CXCL14 prevented the inhibition of IP_3R by 2-APB in MCF7 subclones. Cells were loaded with 5 μmol/L Fluo-3 for 1h. MCF7 (*red curve*) and clone P (*green curve*) were treated with 2 μmol/L thapsigargin (*TG*) to deplete intracellular stores and activate capacitative calcium entry. MCF7 (*brown curve*) and clone P (*blue curve*) were treated with 100 μmol/L 2-APB for 10 min before adding 2 μmol/L thapsigargin. The results of a representative recording of the free Ca^{2+} measured by Fluo-3 fluorescence using flow cytometry as described in Materials and Methods are shown ($n = 3$). *B*, CXCL14 induced Ca^{2+} release from microsomes in a time-dependent manner. Microsomes were incubated with 1 μg CXCL14 protein, and at the

indicated time, they were spun down and the supernatant containing Ca^{2+} was kept to further evaluate Ca^{2+} released. *C*, CXCL14 induced Ca^{2+} release from microsomes in a dose-dependent manner. Microsomes were incubated with up to 1 μg CXCL14 protein for 2 h and then were spun down and the supernatant was used to evaluate Ca^{2+} released. *D*, comparison of Ca^{2+} released from microsomes induced by IP_3, thapsigargin, or CXCL14. Microsomes were incubated with 0.5 or 1 μg of CXCL14 protein, 10 μmol/L IP_3, or 1 0μmol/L thapsigargin for 1 h and then spun down, and the supernatant was used to evaluate Ca^{2+} released. *Columns*, mean of at least three independent experiments; *bars*, SD.

NIH-PA Author Manuscript
NIH-PA Author Manuscript
NIH-PA Author Manuscript